The Republic of the Union of Myanmar
Ministry of Natural Resources and Environmental Conservation

Mineralogy and Geochemistry of Andesites In Popa Area, Kyaukpadaung Township, Mandalay Region

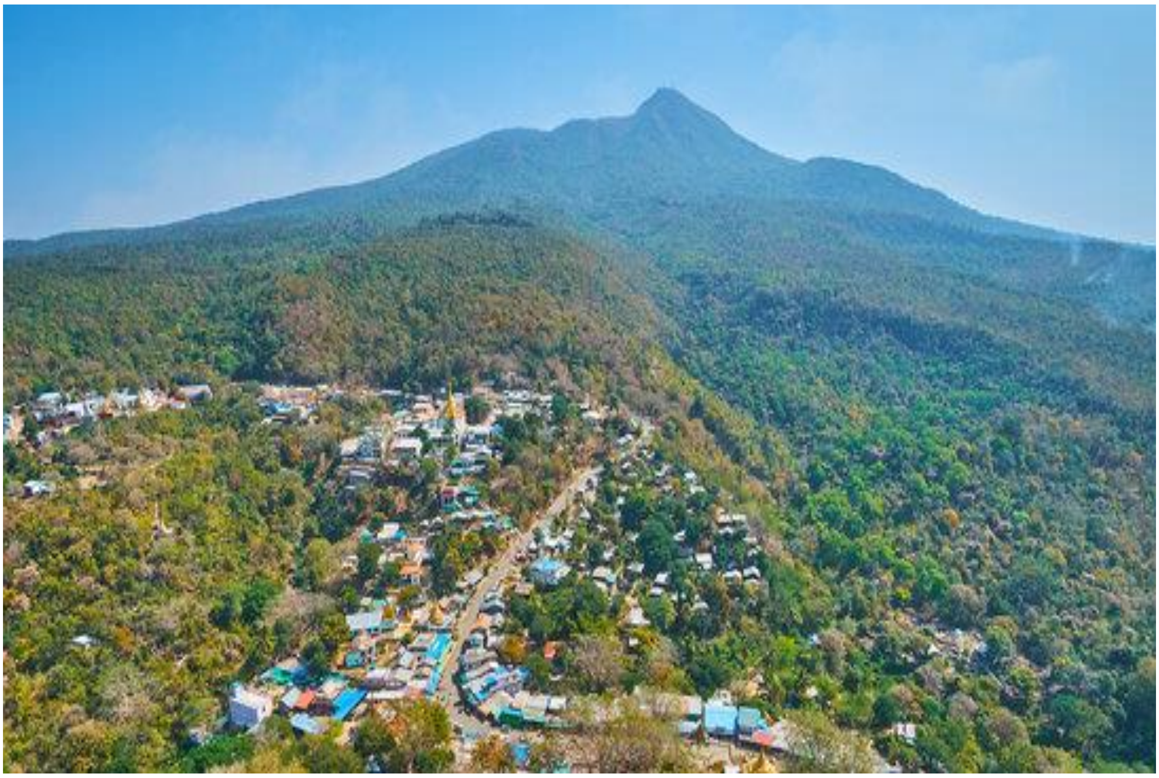

Aye Chan Pyae Kyaw
Deputy Assistant Computer Operator
Myanma Gems Enterprise

March, 2026

Contents

Mineralogy and Geochemistry of Andesites In Popa Area, Kyaukpadaung Township, Mandalay Region

Aye Chan Pyae Kyaw

Deputy Assistant Computer Specialist

Myanma Gems Enterprise

ABSTRACT

The Popa area lies in the Kyaukpadaung Township, Myingyan District in the Mandalay Region. Five distinct morphological features are a volcanic crater, a volcanic plateau, a volcanic neck, a volcanic cone and volcanic slope. Microscopically, the main common textures of the studied samples are porphyritic, glomerophyritic, intergranular, radiate seriate and ophitic to sub-ophitic textures. Based on the modal composition, andesite samples can be divided into augite-hornblende phyric andesite; olivine-augite phyric andesite; hypersthene-hornblende- augite phyric andesite; and augite phyric andesite. Porphyritic texture indicates two phase of crystallization process. Poikilitic texture of augite phenocryst contains other minerals indicates that the order of crystallization can be determined. Plagioclase microcrystalline laths exhibit pilotassitic texture, the sub-parallel arrangement amongst them giving trachytic texture indicate the existence of lava flow processes when rock formation. The regular zoning pattern of plagioclase phenocryst in andesite samples is an indication to changes in magma composition during the crystal growth. Glomeroporphyritic texture occurs as indication of simultaneous crystal growth, in account for heterogeneous nucleation rates amongst crystals. On the basis of geochemical facts and discriminant diagrams, the calc-alkaline nature of andesites from the study area are plotted within the field of volcanic arc and these characters are corresponded with volcanism of this area might be regarded as subduction related.

Keywords: andesites; microscopically; Popa; subduction

မန္တလေးတိုင်းဒေသကြီး၊ ကျောက်ပန်တောင်းမြို့နယ်၊ ပုပ္ပါးဒေသတွင်ရှိသည့် အန်ဒီဆိုက် ကျောက်များ၏ တွင်းထွက်ပညာအရနှင့် ဘူမိဓာတုဗေဒဆိုင်ရာများ

အေးချမ်းပြည့်ကျော်

ဒု-လက်ထောက်ကွန်ပျူတာလုပ်ဆောင်ရေးမှူး

မြန်မာ့ကျောက်မျက်ရတနာရောင်းဝယ်ရေးလုပ်ငန်း

စာတမ်းအကျဉ်း

ပုပ္ပါးဒေသသည် မန္တလေးတိုင်းဒေသကြီး၊ မြင်းခြံခရိုင်၊ ကျောက်ပန်းတောင်း မြို့နယ်တွင် တည်ရှိပါသည်။ ထင်ရှားသောမြေမျက်နှာသွင်ပြင် အနေအထားငါးမျိုးမှာ မီးတောင်ထိပ်ဝ၊ မီးတောင်ကုန်းပြင်မြင့်၊ မီးတောင်လည်တိုင်၊ မီးတောင်ကတော့နှင့် မီးတောင်ဆင်ခြေချောတို့ ဖြစ်ကြသည်။ နမူနာကောက်ယူခဲ့သောကျောက်များကို ဖြတ်ပိုင်းပါးပုံသွေး၍ အဏုကြည့် မှန်ပြောင်းဖြင့် လေ့လာသည့်အခါတွင်အရွယ်အစားသေးသော တွင်းထွက်များအပေါ်မှ အရွယ် အစားကြီးသော တွင်းထွက်များဖြစ်နေခြင်း၊ တွင်းထွက်များအစုလိုက်ဖြစ်ခြင်း၊ လက်ယှက်ထိုး ပုံစံရှိခြင်း၊ ဖြာထွက်နေသော အနေအထားရှိခြင်း၊ အစီအစဉ်အတိုင်း လိုက်ဖြစ်နေခြင်းနှင့် ပလေဂျီရိုကလေ့တွင်းထွက်များသည် ပိုင်ရိုစင်းတွင်းထွက်များအတွင်း၌ ပြီးပြည့်စုံစွာ ပိတ်မိ နေခြင်း(သို့) တပိုင်းတစပိတ်မိခြင်း စသည်တို့ကိုအဓိကကျောက်သားဆင်များအဖြစ် လေ့လာ တွေ့ရှိရပါ သည်။ တွင်းထွက်အမျိုးအစားပါဝင် ဖွဲ့စည်းပုံ ပေါ်တွင် မူတည်၍ အန်ဒီ ဆိုက်ကျောက်များကို အော်ဂိုက်-ဟွန်းဘလင်း၊ အော်လဘင်း-အော်ဂိုက်၊ ဟိုက်ပါ(စ်)သင်း- ဟွန်းဘလင်း-အော်ဂိုက်နှင့် အော်ဂိုက် စသည့် တွင်းထွက်များ ပါဝင်သော အန်ဒီဆိုက် ကျောက်များဟူ၍ ခွဲခြားနိုင်ပါသည်။ ခဲကြီးဝင် ကျောက်သားဆင်သည် ပုံဆောင်ခဲဖြစ်စဉ် အခြေအနေ နှစ်ခု၌ဖြစ်ပေါ်သည်။ ထို့ကြောင့် အော်ဂိုက်တွင်းထွက်များသည် ပလေဂျီရိုကလေ့များထက် ဦးစွာပုံဆောင်ခဲ့ကြောင်း ကောက်ချက် ချနိုင်ပါသည်။ သိပ်သည်း ကျစ်လစ်သည့် ပုံသဏ္ဍာန်နှင့် ပြိုင်တန်းလုနီးပါးဖြစ်ပေါ်နေသော ပလေဂျီရိုကလေ့များသည် ကျောက်ဖြစ်စဉ်ကာလအတွင်း ချော်ရည်စီးကြောင်း ဖြစ်စဉ် ဖြစ်ပေါ် ခဲ့သည်ကို ပြသနေပါသည်။ ထို့အပြင် အရွယ်အစား ကြီးသည့် ပလေဂျီရိုကလေ့တွင်းထွက်များတွင် အရစ်လိုက်အကွက်များ ပါရှိခြင်းသည် ပုံဆောင်ခဲဖြစ်ပေါ်နေစဉ် အတောအတွင်း၌ ချော်ရည် ဖွဲ့စည်းပုံပြောင်းလဲခြင်း ဖြစ်ခဲ့သည်ကိုညွှန်ပြနေပါသည်။ အမျိုးအစားမတူသော တွင်းထွက် ဖြစ်ပေါ်မှုနှုန်း ဆက်တိုက်ဖြစ်သောကြောင့် တွင်းထွက်များ အစုလိုက် ဖြစ်တည်နေသော ကျောက် သားဆင် တို့ကိုလည်း လေ့လာ တွေ့ရှိပါသည်။ ဘူမိဓာတုဗေဒအချက် အလက်များနှင့် ဖော်ပြ သည့်ဇယားပုံများပေါ်တွင် အခြေခံ၍ လေ့လာသောဧရိယာတွင် တည်ရှိသော ကတ်-အယ်လ် ကာလိုင်း အန်ဒီဆိုက် ကျောက်များသည် မီးတောင်ကျွန်းတန်းနယ်ပယ်တွင် ကျရောက်ပြီး ယင်းအချက်အလက် များအရ ထိုဧရိယာရှိမီးတောင်ဖြစ်စဉ်သည် စိုက်ဝင်မှုနှင့်ဆက်စပ် နေသည် ဟု သတ်မှတ် ရပါသည်

Mineralogy and Geochemistry of Andesites In Popa Area, Kyaukpadaung Township, Mandalay Region

1. Introduction

The Popa area lies in the Kyaukpadaung Township, Myingyan District in Mandalay Region (Figure 1.1). It is also located about 8 miles northeast of Kyaukpadaung. It is situated between latitudes 20°54′00″N to 20°58′00″N and longitudes 95°11′00″E to 95°15′00″E. It is bounded by vertical grids 260 to 340 and horizontal grids 100 to 190 in UTM map sheet no.2095 01. It is about 8.5 kilometers long in the N-S direction and 7.5 kilometers wide E-W direction and hence, the total coverage of the area covers approximately 63.75 square kilometers (24.6 square miles).

Mt. Popa is a stratovolcano in central Myanmar and is located within and protected by Mt. Popa National Park. The name Popa is believed to derive from the Sanskrit word puppa, meaning flower. Mt. Popa is a popular destination for local people, and there is much history and many legends involving the mountain. A volcanic plug, called Taung-Kalat, at the western foot of Mt. Popa is a prominent landmark. It is one of the most famous religious sites in Myanmar and several thousand people visit each year for religious and tourism purposes.

The Popa area locating in the central Myanmar attracts everybody for its fantastic and majestic landscape which is mainly originated by volcanogenic origin. The scenic Mt. Popa (locally called Taungmagyi) and lovely volcanic stock (Taunggalat) are prominent forms which evident the central eruption type. Five distinct morphological features are volcanic crater, volcanic plateau, volcanic neck, volcanic cone, volcanic slope.

Mt.Popa appears as a great mountain as it dominates the surrounding flat plain. It is an ancient volcano and is only about 3000 feet high from its base. Mostly, the volcanic vent is an elevated upland forming rugged terrain, covering fairly vegetation. Mt.Popa is a stratovolcano with 1 mile in diameter from west to east and the average depth is 2000 feet. The inner slope of the crater is steeper than the outer slope. Originally, its crater may have assumed a circular shape. Due to the final paroxysmal outburst (violent explosion), the northern flank of the older crater rim was blown away and retained as a northward opening crater forming a horse-shoe-shaped crater. The final stage of volcanism occurred in Mount Popa could be a "Vesuvian" type of volcanic eruption. Magma violently explored form the stratocone and lava flowed outward in some distance. Ngayangon and Taungbaw flows indicated this explosion. The most prominent peaks in the crater rim are Hmanpya Taung (4981') at southeastern part, Sabapon Taung (4801') at southwestern rim and Saemon Taung (4502') at the western rim. On the southwestern slope Taunggalat (2417') is a precipitous peak which is the in filled neck of a subsidiary volcano.

This area under the present investigation is situated in the Central Cenozoic belt that is underlain by various orderly successions of Cenozoic sedimentary strata and some igneous and metamorphic rocks. Chhibber (1934) suggested that Mt. Popa could have had an eruption 442 BCE. Belousov et al. (2018) mentioned that the latest period of volcanic activity on Mount Popa took place at the beginning of the Holocene. It included several mild explosive eruptions and Mt. Popa should be listed as an active volcano.

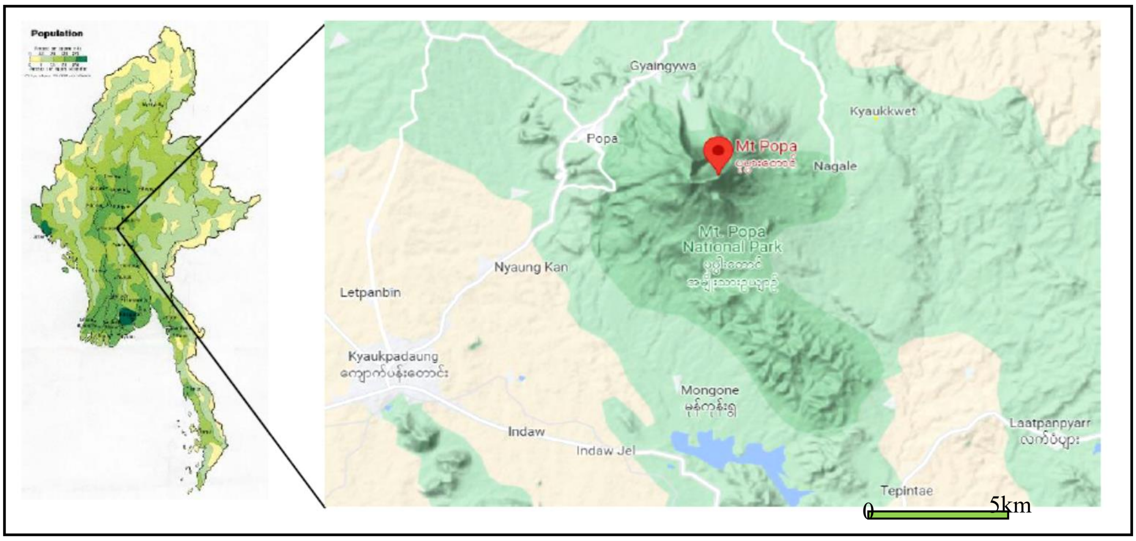

Figure 1. Location map of the Popa area, Mandalay Region

2. Objectives

The main purpose of this investigation reflects the petrogenesis of andesites from Popa area based on mineralogy and geochemistry. The present investigation will focus on the following objectives.

(a) To investigate the petrographic features of the andesites of the Popa area.
(b) To interpret the geochemistry and petrogenesis of the andesites exposed in the popa area.
(c) To investigate the tectonic setting of rocks of the Popa area.

3. Materials and Methods

3.1 Materials

UTM map no.2095 01 was used as guide map in the field. Outcrop mapping was carried out by conventional means by using Brunton Compass, Global Positioning System (G.P.S), a geological hammer, and tape. About twenty (20) representative whole rock samples were collected for the purpose of petrographic studies.

3.2Methods

3.2.1 Field Method

Before going to the field, a literature survey, aerial photo, satellite image interpretation, and collection of maps were taken. Rocks and mineral samples were collected for detailed mineralogical and geochemical analyses. Topographic features, exposures, structures, etc. were taken photographs in the field. The traverses especially along the car road and stream were made by many measurements. All observed and measured data along traverse lines were plotted on the base map in the field.

3.2.2 Laboratory Method

Represented samples were selected from the andesites of the study area. About (20) thin sections were prepared in the laboratory for the petrographical and mineralogical studies. Petrographic analysis of andesites will be determined by using the polarizing microscope. According to the petrographic studies, (8) samples of unaltered rocks were selected for chemical analysis. The selected samples were crushed and powdered using pulverizer. These powdered samples were used for measuring the major and trace elements by Energy Dispersive

X-ray Fluorescence (EDXRF). Moreover, results of major and trace element composition have been plotted to deduce the magma composition, the origin of crystallization, the fractionation process, and possible tectonic setting by using Geochemical Data Toolkit (GCDkit) software.

4. Results

Microscopically, the main common textures of the studied samples are porphyritic, glomerophyritic, intergranular, ophitic to sub-ophitic, radiate and seriate textures. Based on the modal composition of minerals, andesites of the study area can be divided into (1) augite-hornblende phyric andesite; (2) olivine-augite phyric andesite; (3) hypersthene-hornblende-augite phyric andesite; and (4) augite phyric andesite.

The most common andesite of the study area is the augite-hornblende phyric andesite. It is made up of plagioclase, hornblende, pyroxenes, olivine, opaque minerals (mainly iron oxides) and secondary minerals such as iddingsite.

Table 1. Modal composition in vol% of andesites from the study area

Sample No.	**A1**	**A2**	**A3**	**A4**	**A5**	**A6**	**A7**	**A8**	**A9**	**A10**
Plagioclase	15	20	10	16	14	12	5	7	4	14
Orthoclase	-	-	-	2	3	2	2	-	1	-
Nepheline	-	3	-	-	-	-	2	3	2	-
Augite	22	10	25	3	5	3	19	20	21	25
Hornblende	3	4	2	20	23	25	4	5	3	4
Hypersthene			2	5	2	-	-	-	-	2
Olivine	2	-	-	-	2	2	2	3	2	-
Opaque & secondary minerals	2	1	1	2	2	1	1	2	2	1
Groundmass	56	62	60	52	50	55	66	60	65	54
Total	100	100	100	100	100	100	100	100	100	100

4.1 Plagioclase

Under the microscope, the plagioclase crystals are the predominant minerals forming up to 60% and occur both in phenocrysts and microcrystalline groundmass. They are subhedral to euhedral, tabular crystals in phenocrysts and lath-liked microcrystals in groundmass. The size of plagioclase ranges from 0.2mm to 3mm in length. Moreover, oscillatory and other types of zoning occur in plagioclase (Figure 2). The zonal arrangement of minute melt inclusions in plagioclase suggests that the several stages in the growth of plagioclase crystals. Crystal clots of plagioclase, augite and olivine forming glomeroporphyritic texture are commonly observed in some samples. In some slides, plagioclase crystals in groundmass give subparallel alignment, trachytic texture (Figure 3).

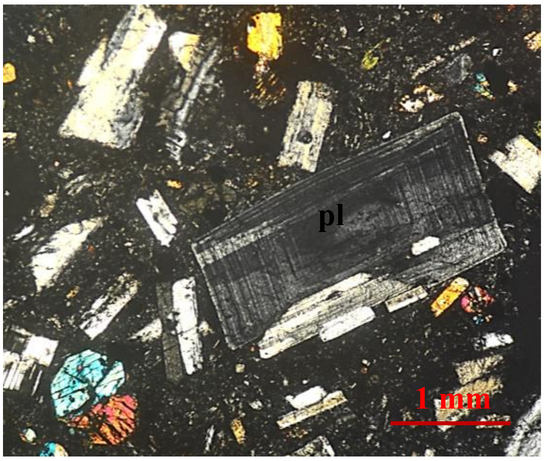

Figure 2. Photomicrograph of augite phyric andesite showing the oscillatory zoning in plagioclase (XPL magnification,4×)

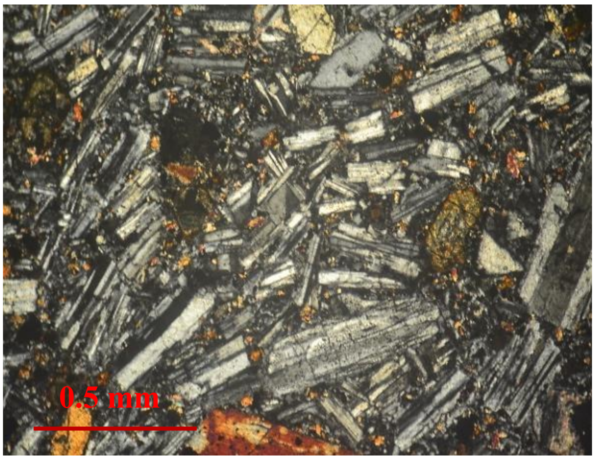

Figure 3. Photomicrograph of olivine augite phyric andesite giving trachytic texture with subparallism of plagioclase laths. (XPL magnification, 4×)

4.2 Orthoclase

Rarely, orthoclase occurs as phenocrysts in some samples with plagioclase and hornblende. It is found as subhedral form, colorless (cloudy due to alteration), first order grey interference color and simple and baveno twinning is present (Figure 4 & 5).

4.3 Hornblende

Hornblende occurs as major amphibole mineral in andesites of the study area. Hornblende has euhedral to subhedral long prismatic form. The average grain size is 0.5 to 3mm in length. It is high relief and two sets of cleavage. The basal section gives 2-set of cleavage cut nearly $60^{\circ}/120^{\circ}$ (Figure 6) and symmetrical extinction can be seen frequently. Zoning can be occurred and simple twin is also present. The maximum interference color is third order reddish brown color. Most of them are oxo-hornblende with pale yellowish brown to dark chestnut brown pleochroism. The black iron-oxides often seen around the edge of Oxo-hornblendes can be found frequently (Figure 7).

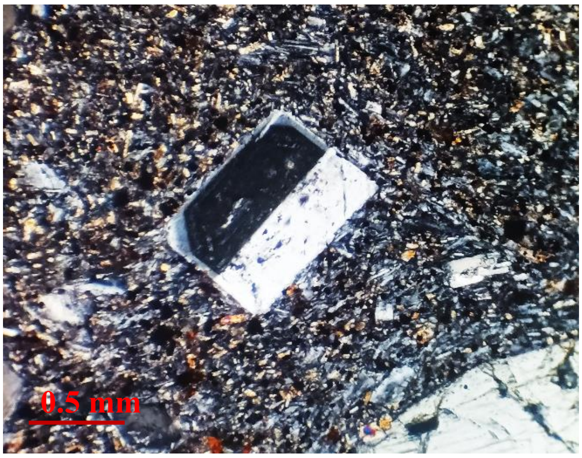

Figure 4. Photomicrograph showing simple twins in orthoclase of augite-hornblende phyric andesite (XPL magnification, 10×)

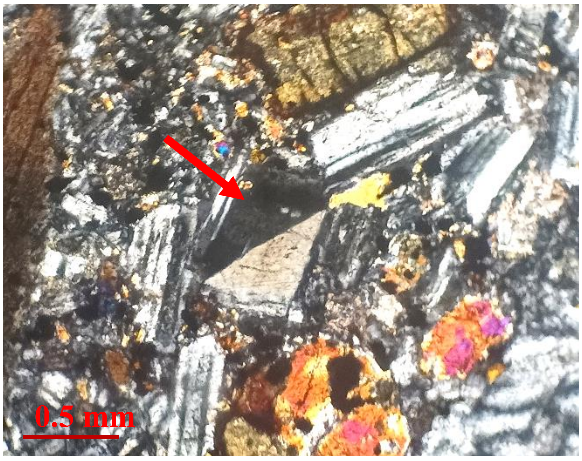

Figure 5. Photomicrograph showing Baveno twins in orthoclase (arrow) in olivine-augite phyric andesite (XPL magnification, 10×)

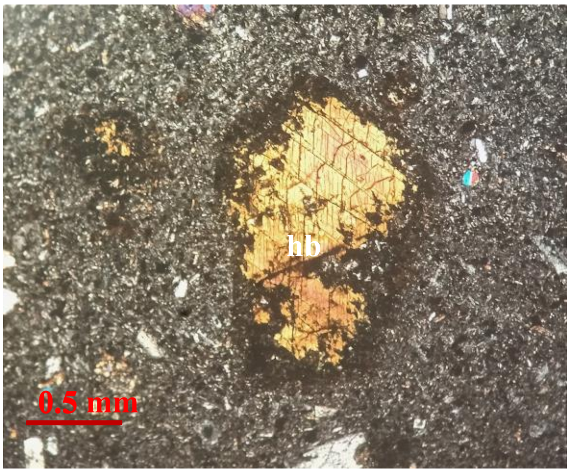

Figure 6. Photomicrograph of basal section of hornblende having 2-set of cleavage cut nearly 60°/120° in augite-hornblende phyric andesite (XPL magnification, 4×)

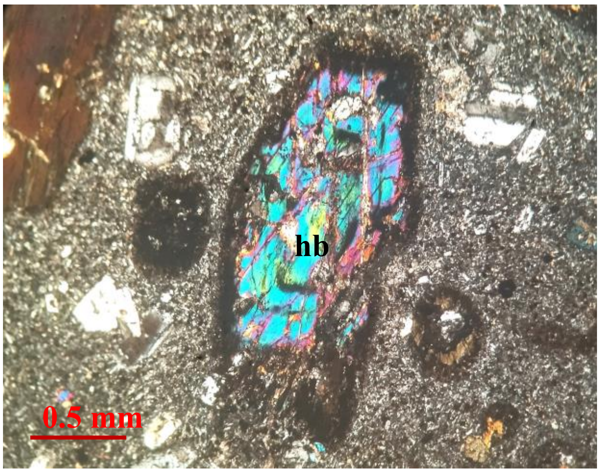

Figure 7. Photomicrograph of augite-hornblende phyric andesite showing iron-oxide rim in euhedral to subhedral Oxo-hornblende. (XPL magnification, 4×)

4.4 Augite

Augite occurs mostly as megacryst or phenocryst, microphenocryst as well as in groundmass. It is eight-sided euhedral to subhedral, up to 1.5mm in diameter and fresh prismatic crystal. It has colorless or pale green in color, high relief and pleochroic from light green to green color. It also gives well defined cleavage of 2-set cutting at right angle (Figure 8). Most of the longitudinal sections show inclined extension with higher degree and symmetrical extinction can be seen in basal section. It is noteworthy that augite in andesite of the study area has sector zoning (Figure 9), oscillatory zoning (Figure 10) and twinning (Figure 11). Numerous inclusions in augite showing poikilitic texture can be seen in olivine-augite phyric andesite.

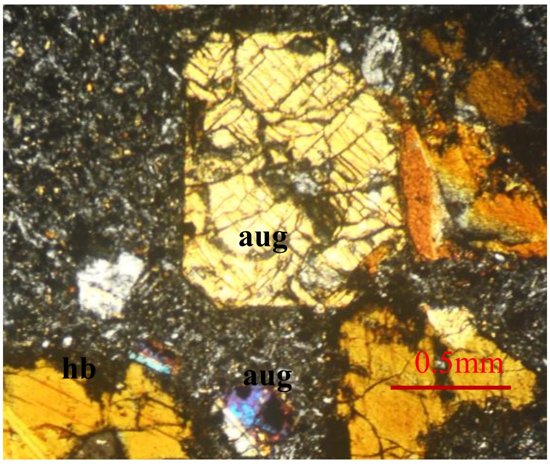

Figure 8. Photomicrograph showing the subhedral augite with well-defined 2-set of cleavage cutting at right angle in augite of hornblende phyric andesite (XPL magnification, 4×)

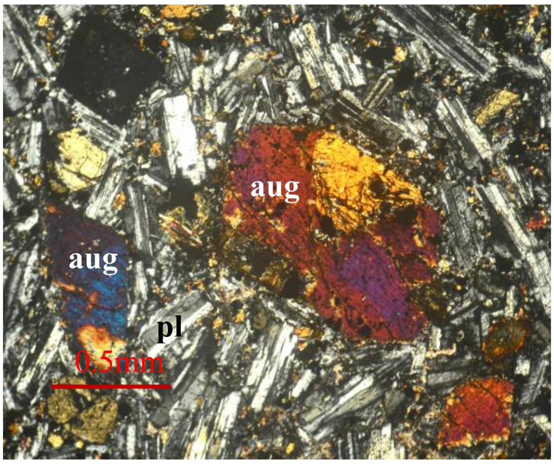

Figure 9. Photomicrograph showing the sector zoning in augite of olivine augite phyric andesite (XPL magnification, 4×)

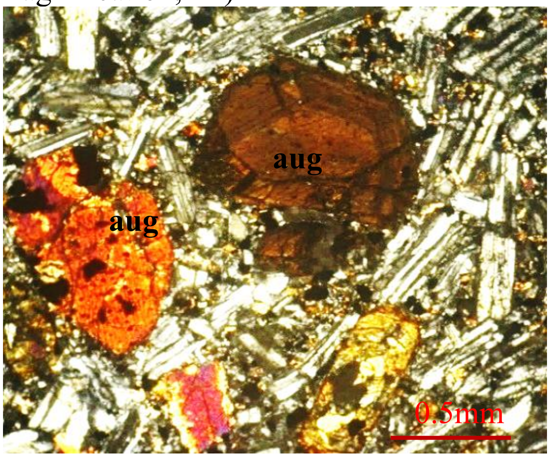

Figure 10. Photomicrograph showing the oscillatory zoning in augite of olivine-augite phyric andesite (XPL magnification, 4×)

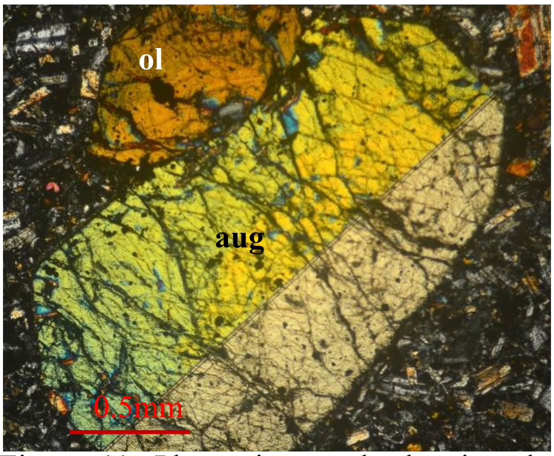

Figure 11. Photomicrograph showing the simple twinning of euhedral augite (aug) crystal in augite phyric andesite (XPL magnification, 4×)

4.5 Olivine

Olivine occurs as minor amount in the andesites of the study area. Petrographically, most of the olivine gives six-sided euhedral to subhedral phenocrysts, colorless, high relief and parallel extinction. In some samples, olivine is characterized by sector and oscillatory zoning (Figure 12). It also occurs in association with plagioclase, augite giving glymeroporphyritic texture (Figure 13).

4.6 Hypersthene

Hypersthene occurs as phenocrysts in some samples (Figure 14). It has nearly similar characteristics to augite, it tends to be lighter in color, characteristic pleochroism from green to pink, lower order of interference color, and has parallel extinction. Black opaque inclusions are found in some hypersthene phenocrysts.

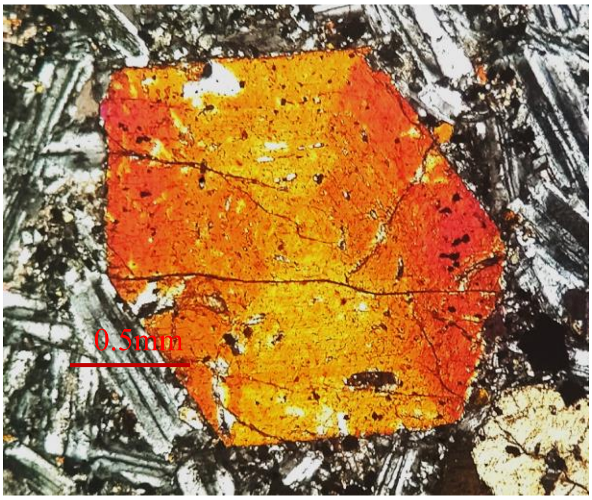

Figure 12. Photomicrograph showing the six-sided euhedral olivine with sector and oscillatory zoning in olivine-augite phyric andesite (XPL magnification, 10×)

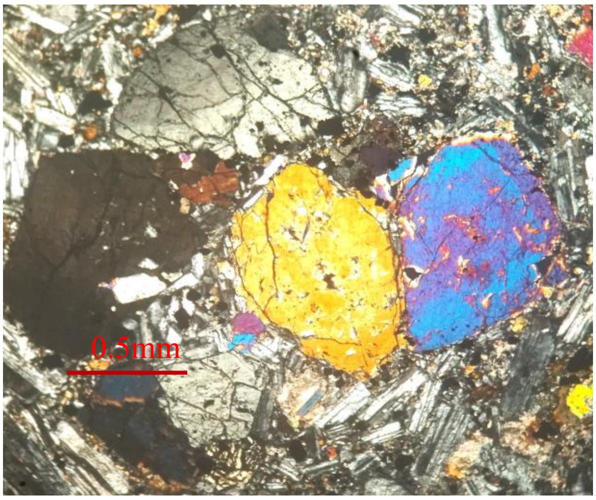

Figure 13. Photomicrograph showing glomerocrysts of olivine and augite in olivine-augite phyric andesite (XPL magnification, 4×)

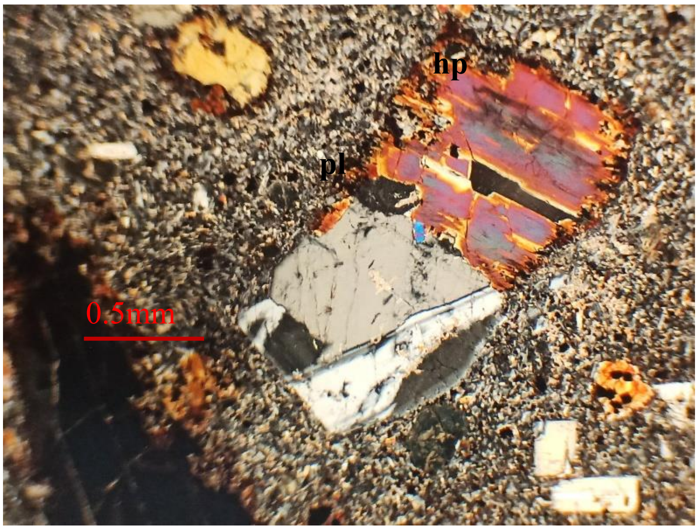

Figure 14. Photomicrograph of augite-hornblende phyric andesite showing the cluster of hypersthene (hp) and plagioclase (pl) phenocrysts. (XPL magnification, 4×)

4.7 Opaque Mineral

Under microscope, magnetite is found as black opaque, anhedral grain as microphenocryst and groundmass. In addition to magnetite also formed as inclusion in large phenocrysts.

4.8 Secondary Mineral

Iddingsite, clay minerals and chlorite are found as secondary minerals in andesites of the study area. Iddingsite occurs in the fracture and boundary of olivine crystals. Yellowiah brown color clay minerals can be found rarely as groundmass and alteration product from plagioclase. Deep green chlorite are anhedral forms as alteration product of hornblende.

4.9 Geochemistry

In order to geochemical studies, (8) andesite samples as much as possible unaltered and minimum weathering and secondary streak which covered characteristics of the area rocks were selected and transferred for powdering with pluverizer. These powder samples were chemically analyzed for major oxides and trace elements by using Energy Dispersive X-Ray Fluorescence (EDXRF). The analytical data were plotted in classification and tectonic discrimination diagrams by using GCDkit version 2.3 software.

Based on geochemical compositions, the studied samples have shown the character of andesite and basaltic andesite which is predominantly calc-alkaline in nature. Andesites and basaltic andesites are characterized by SiO_2 (52.42- 56.29%), Fe_2O_3 (6.71-7.89%), Al_2O_3 (18.98-22.50%), MgO (2.24-3.73%), CaO (8.29-10.86%), Na_2O (2.32-3.50), K_2O (1.14-1.55), and TiO_2(0.72-0.91). The analytical results of trace elements show some significant values viz. Ba (2060-2590ppm), Cr (95.79- 143.68ppm), Rb (10-54.86 ppm), Sr (846-1057ppm), V(120-190ppm), Y(10ppm) and Zr (20-60ppm) (Table 2).

The analytical results of the studied samples are plotted in Total Alkali-Silica (TAS) diagram which indicate that the most of samples fall in the andesite and basaltic andesite fields (Figure 15). SiO_2 versus Zr/TiO_2 diagram of Winchester and Floyd (1977) is used which come under the andesite and andesite-basalt fields (Figure 16).

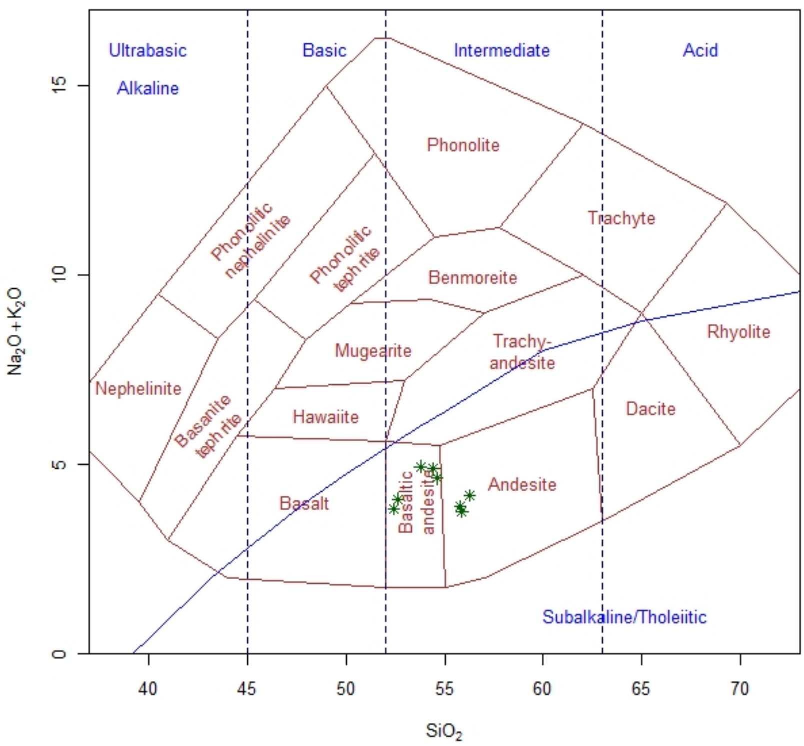

Figure 15. TAS diagram, after (Cox et al., 1979), showing the andesite samples located within andesite to Basaltic andesite field

Table 2. Geochemical data for representative andesites of the Popa area

Samples	A1	A2	A3	A5	A6	A7	A8	A11
Major oxides (%)								
SiO_2	54.448	54.625	53.772	56.286	55.806	55.887	52.422	52.617
TiO_2	0.724	0.752	0.907	0.788	0.919	0.836	0.81	0.757
Al_2O_3	19.079	18.797	21.502	18.7	17.984	18.713	21.434	21.006
Fe_2O_3	7.342	7.778	7.657	7.302	7.895	7.291	6.715	6.991
MnO	0.116	0.141	0.144	0.142	0.156	0.135	0.125	0.159
MgO	3.738	2.982	2.243	2.633	3.466	2.856	3.601	2.894
CaO	9.18	9.758	8.296	9.535	9.241	9.942	10.417	10.862
Na_2O	3.5	3.223	3.382	2.621	2.801	2.613	2.324	2.691
K_2O	1.38	1.406	1.56	1.558	1.091	1.14	1.492	1.393
P_2O_5	0.352	0.421	0.383	0.279	0.511	0.466	0.514	0.472
Total	99.859	99.883	99.846	99.844	99.87	99.879	99.854	99.842
Trace elements (ppm)								
Rb	10	27.432	45.72	10	54.864	10	54.864	27.432
Sr	1006.26	845.6	1090.82	1116.19	904.79	854.05	1006.26	1057
Zr	50	20	60	30	30	40	40	50
Ba	2510	2450	2600	2060	2300	2590	2750	2700
Cr	123.156	95.788	136.84	136.84	123.156	109.472	143.682	102.63
Y	10	8	9	10	8	10	7	6
Hf	30	25	35	20	30	20	30	35
La	590	550	530	540	620	610	630	570
Ce	320	200	290	180	260	320	190	300
Eu	500	520	440	460	480	540	530	555
V	180	190	170	120	130	170	160	150
CIPW-Norms (wt%)								
Or	9.13	9.26	10.23	9.90	7.35	7.75	10.08	9.48
Ab	29.48	27.15	28.48	21.86	23.60	22.00	19.95	23.15
An	34.33	34.74	38.82	36.44	35.38	37.97	40.95	38.49
Di	7.46	9.16	-	7.22	6.00	6.95	6.92	10.49
Hp	14.46	12.32	14.65	14.06	15.03	12.30	13.78	10.75
Ne	-	-	-	-	-	-	-	-
Ol	-	-	-		-	-	-	-
Hm	-	-	-	-	-	-	-	-
Ap	0.83	0.99	0.90	0.65	1.20	1.09	1.23	1.13
Pf	-	-	-	-	-	-	-	-
Il	1.37	1.42	1.71	1.48	1.74	1.58	1.56	1.46
Mag	1.27	1.35	1.33	1.25	1.37	1.26	1.19	1.24
Zr	0.01	0.00	0.01	0.01	0.01	0.01	0.01	0.01

Or: Orthoclase; Ab:Albite; An:Anorthite; Ol: olivine; Di: Diopside; Ap: Apatite; Il: Ilmenite; Hm: Hematite; Pf; Perovskite; Ne: Nephaline; Hp: hypersthene; Mag: magnetite; Zr: zircon

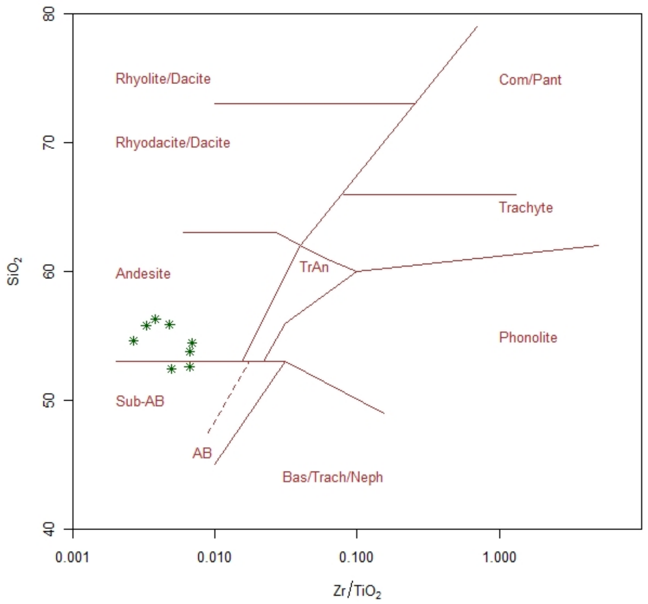

Figure 16. Rock classification diagram modified from Zr/TiO_2 vs. SiO_2 (Winchester and Floyd, 1977)

The total alkali vs. silica diagram (Irvine and Baragar, 1971) show that the andesite samples dominantly plot within subalkaline field (Figure 17). These results have been documented by previous authors such as Sano (2022) and Hla Min (2022).

Irvine-Barager Discriminant diagram (1971) used to determine series of magma that formed andesites of the study area. Irvine-Barager diagram discriminate magma series between tholeiitic and calc-alkaline series. Geochemical compound that used in this diagram is total FeO (Fe_2O_3+FeO), Na_2O+K_2O and MgO (in wt%). Data plotted on the AFM diagram (Figure 18) clearly indicate that almost all of the andesites fall in the field of calc-alkaline series. So, it can be interpreted that calc-alkaline nature of andesites from the study area is genetically related to the subduction related plate tectonic process.

Whereas Al-Mg-Fe^T+Ti ternary diagram (after Jensen1976), most of the studied samples plotted within the andesite field of calc-alkaline series (Figure 19).

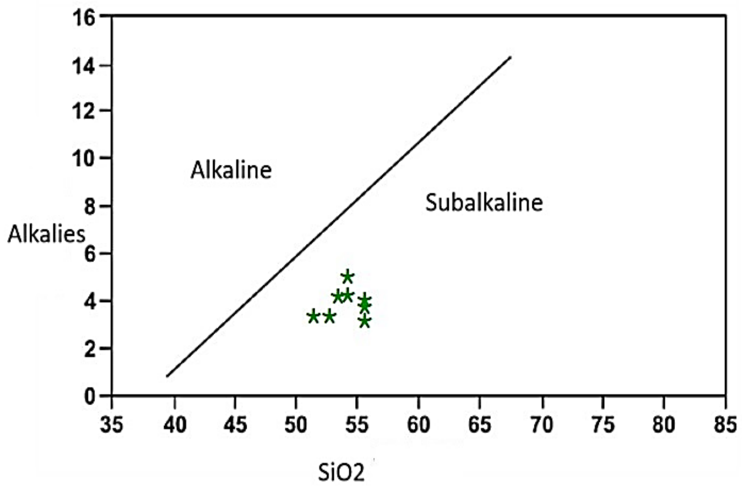

Figure 17. Total alkali vs. silica diagram showing all samples fall into subalkaline Series (after Irvine and Barager, 1971)

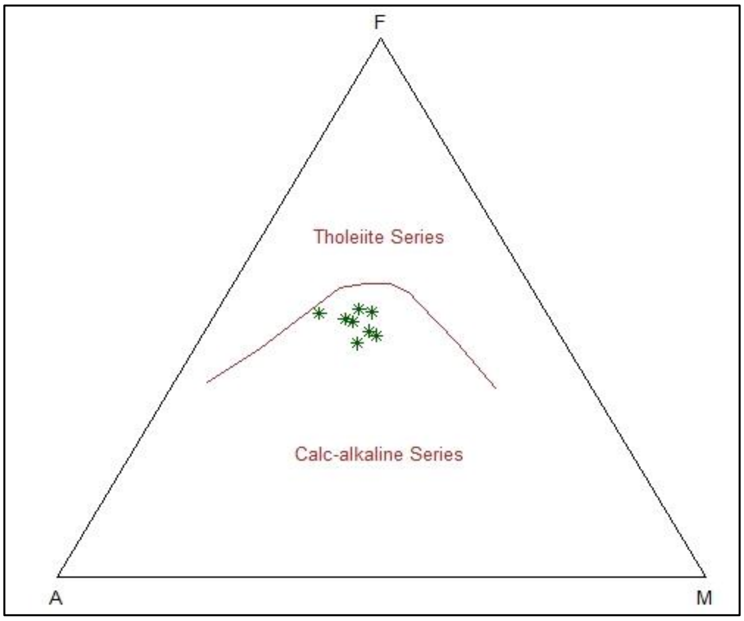

Figure 18. AFM ternary diagram showing all samples fall into Calc-alkaline Series (after Irvine and Barager, 1971)

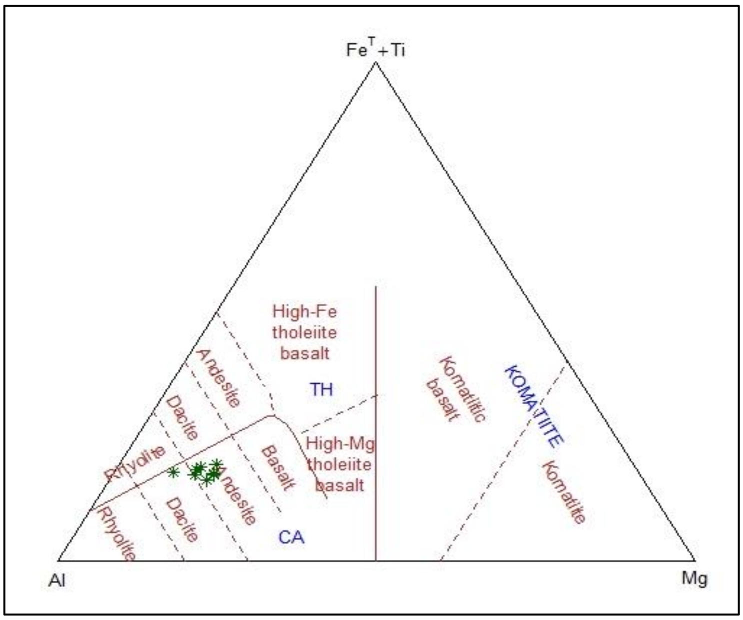

Figure 19. Al-Mg-Fe^{T}+Ti ternary diagram (after Jensen1976) showing the studied samples plotted in the andesite Calc-alkaline field

4.10 Geotectonic Implication

The geochemical analysis of major and trace elements for studied andesite samples was used to construct the discriminate diagrams, which help to classification, nomenclature and interpretation of the tectonic setting of andesites from Popa area.

Pearce (1977) determined the origin of magma based on a comparison of the percentage weight value of oxides K_2O, TiO_2, and P_2O_5. Based on this diagram, it can be seen the origin of the rock-forming magma of andesite of the study area, whether interacting with continental crust or oceanic crust. Based on K_2O, TiO_2, and P_2O_5, origin of andesites related to continental crust (Figure 20).

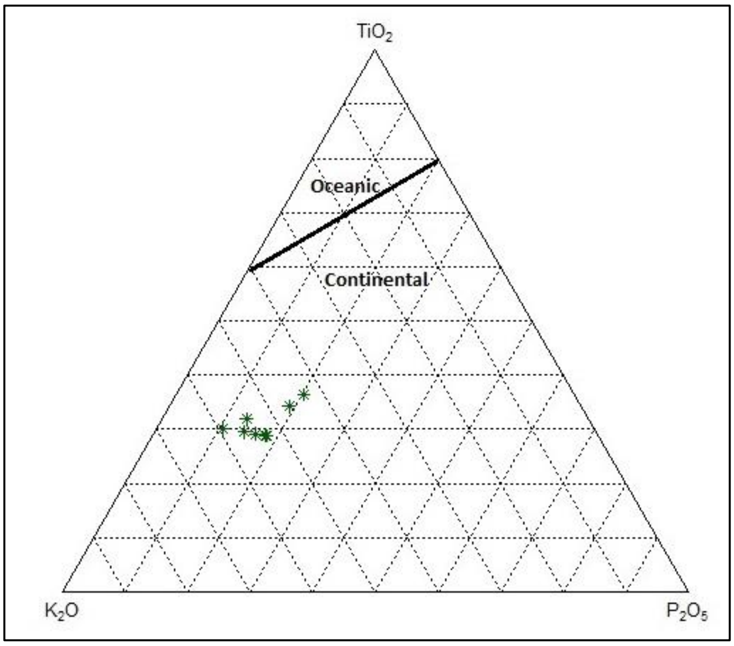

Figure 20. Magmatic series of studied andesites based on diagram of Pearce (1977).

Mullen (1983) diagram of the origin of magma is based on consideration of the weight percentage value of compounds TiO_2, 10xMnO, and 10xP_2O_5. Based on this analysis, it can be seen the origin of magma of a basaltic material, whether it comes from mid oceanic ridge, island arc or oceanic crust. Island arc itself can be divided into tholeiite, alkaline and boninite type. Oceanic crust can be divided into tholeiite and alkaline type. According to diagram of TiO_2, 10xMnO, and 10xP_2O_5 (Pearce, 1977; Mullen, 1983), all analyzed andesite samples related to Island Arc-Calc Alkaline Series (Figure 21).

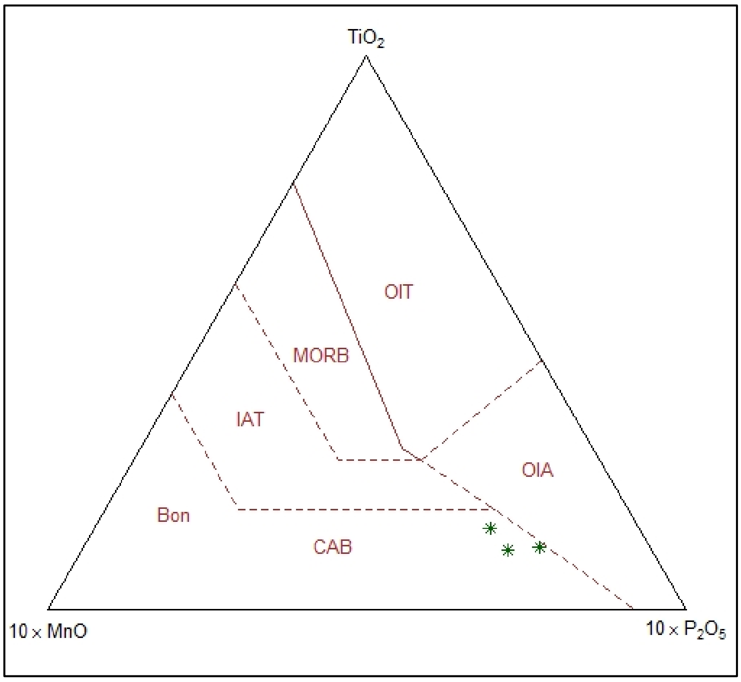

Figure 21. Tectonic setting classification based on TiO2-MnOx10-P2O5x10 (after Mullen, 1983) showing the studied samples were formed in the Calc-Alkaline Basalt (CAB) setting

Tectonic setting classification based on Zr versus Ti (Pearce, 1982) show that the igneous rocks were formed in the volcanic arc, mid-oceanic ridge and within plate settings. The studied andesites have been erupted in volcanic arc setting indicated by tectonic discrimination diagram including Zr versus Ti (Pearce,1982) (Figure 22). In the Zr versus Y diagram after Muller and Gorves (1997), all the samples plotted within the arc related fields (Figure 23).

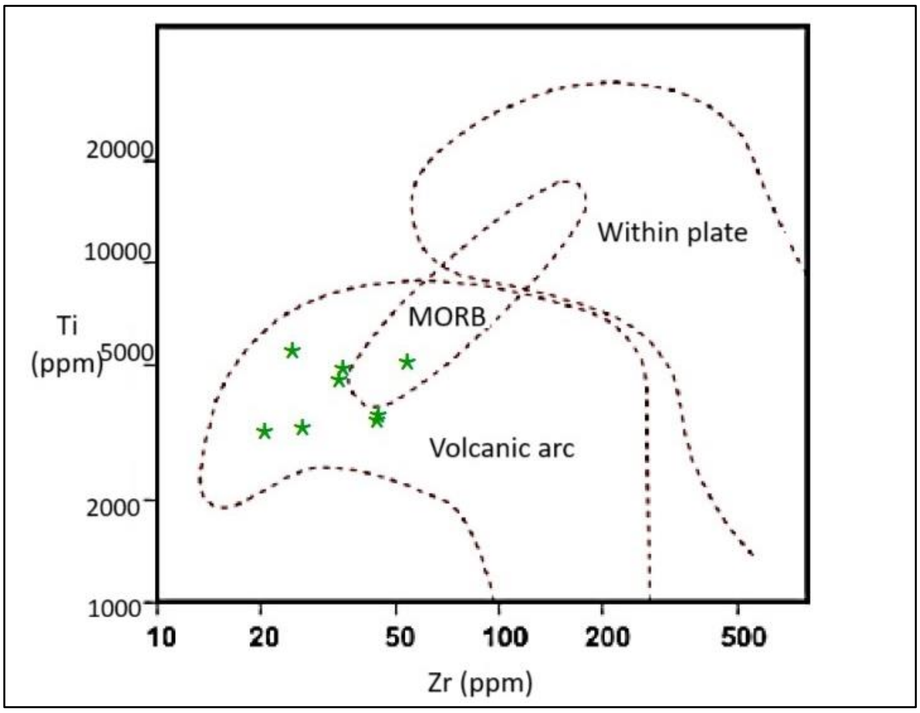

Figure 22. Geotectonic context of the andesites of Popa area according to Ti vs. Zr (after Pearce, 1982)

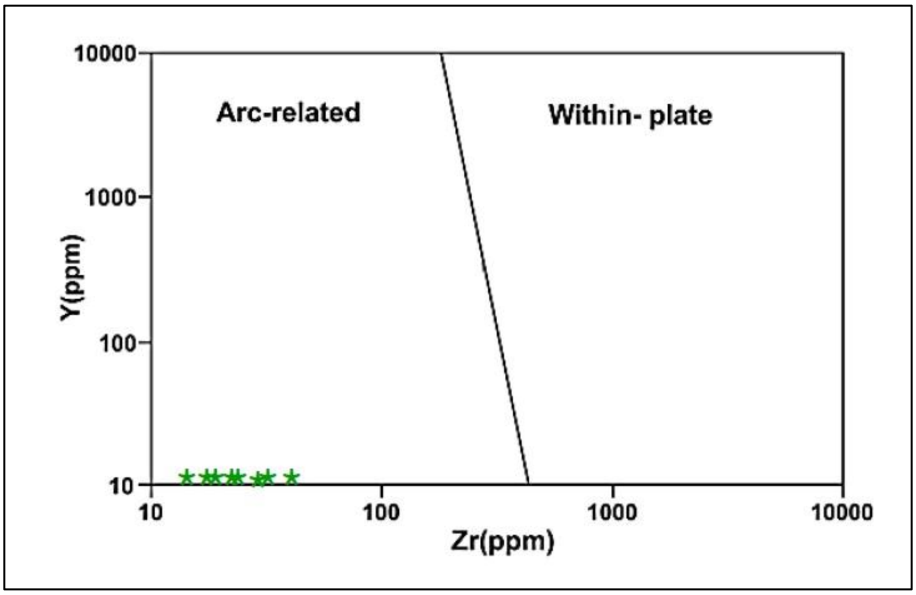

Figure 23. Determination of tectonic environment of the andesites of Popa area according to Y vs. Zr (after Muller and Groves, 1997)

5. Discussion

5.1 Petrographic and Geochemical Characteristics in Magmatic Processes Interpretation

Petrographic analysis of thin section has identified more detailed textural relationship that is essential to understand the origin of rocks. Mostly andesites in the study area are porphyritic andesite with more than 40% phenocrysts embedded in volcanic glass and microlite groundmass. Porphyritic texture indicates two phases of crystallization process. First phase is formed in the deeper location while the second phase is resulted by rapid cooling during volcanism activity when magma is rising up. The phenocryst in igneous rock tend to formed by slower crystallization in the magma chamber that the modification processes are inevitable.

The regular zoning pattern of plagioclase phenocryst in andesite samples is an indication to changes in magma composition during the crystal growth. Magma differentiation also indicated by the presence of oscillatory zoning texture (see Figure 2). This zoning texture is formed due to pressure and temperature change during magma raising and volatile release during magmatic eruption which causes plagioclase compositional differentiation (Fenner, 1926 in Johannsen, 1939). Plagioclase microcrystalline laths exhibit pilotassitic texture, the sub-parallel arrangement amongst them giving trachytic texture and becomes a reference in telling the existence of lava flow processes when rock formation (see Figure 3). Flow texture in andesite of the study area reflects that the magma was moving at the time of solidification.

The iron-oxides are often seen around the edge of Oxo-hornblendes result from resorption effects (see Figure 3.17). Such crystals probably crystallized as typical magnesio- or ferro-hornblende but were transformed during later stage oxidation (Deer et al., 2013). According to Suhada and Dyash Hastuti (2019), the presence of pyroxenes in studied andesites show that this rock freezing process starts at a fairly high temperature which is around 1000 °C to 1200° C. However, the presence of hornblende that coexist with pyroxenes indicate that there is a fairly rapid temperature in change in this rock formation.

In addition, poikilitic texture of augite phenocryst contains other minerals indicates that the order of crystallization can be determined, which the enclosed crystal must be crystallized earlier than the enclosing crystal (oikocryst). Olivine-augite phyric andesite having intergranular textures with grains of augite, olivine and magnetite between plagioclase laths pointed out that most crystal nucleate and grow at the same rate. Ophitic and sub-ophitic texture of augite-hornblende phyric andesite indicates the coprecipitation of plagioclase with pyroxene.

In olivine augite phyric andesite of the study area, the cluster of phenocrysts with plagioclase, augite and olivine often formed crystal aggregates, also called glomerocryst, (see Figure 13) as known to be glomeroporphyritic texture which indicates crystal fractionation by crystal settling since the density of the glomerocryst is an average of that of its constituent phase.

Geochemical anomalies in SiO_2 at two basaltic andesite samples shows 52%, while the other andesite samples at 56-57%. This could indicate that the two samples are more basic than others, as one of evidence of fractional crystallization process. Moreover, Al_2O_3, Na_2O and K_2O are low in basaltic andesite compared to those of same oxides in andesites. On the other hand, TiO_2, Fe_2O_3, MgO, CaO and total lesser extent P_2O_5 contents are high in basaltic andesite compared to andesites. The decrease in TiO_2, MgO, CaO and P_2O_5 reflects the crystallization of iron-titanium oxide minerals. The high contents of SiO_2, Al_2O_3, Na_2O and K_2O in differentiated lavas suggested accumulation of alkali feldspar crystals in these rocks.

Most of the previous authors pointed out that the volcanism in Popa area might be regarded as subduction related.Maung Thein (2000) postulated the subduction of the Indian

Plate under the overriding Burma Plate, might continue, till the Holocene time, along the Rakhine off-shore region as suggested by the formation of an outer magmatic arc (central volcanic line) and renewed volcanism (mainly andesites and basalts) along central Igneous line (Mt. Popa and Twindaung) during Pleistocene and Early Holocene. Mt.Popa and Twindaung overlie a well-defined Wadati- Benioff plane 120-140 km deep (Guzman- Spezials and Ni, 1996; Satyabala, 1998 in Maury et.al, 2004). Mt.Popa volcanic area (including the study area) occupies the rock association of basalt, basaltic andesite, latite and rhyodacite (Aung Moe, 1980; Stephenson & Marshall, 1984). The two groups of lava (Kyaukpadaung and Mt. Popa) are regarded as a single petrographic suite in which several continuous and discontinuous mineral reaction series are recognized.

The more siliceous lavas as the study area may have been derived by fractional crystallization of such magmas at crustal levels. The magmatism is attributed to the waning stages of orogeny as eastward subduction of the Indian plate beneath Burma gave way to strike-slip movement, associated with the Andaman Sea spreading center. Within the tectonic model, magmas were probably generated by hydrous mantle melting above dehydrating oceanic crust of the subduction zone (Stephenson & Marshall, 1974; Hla Min, 2022; Sano et al., 2022).

According to the above mention geochemical facts and discriminant diagrams point out that all the studied samples fall within the field of volcanic arc. These characters are corresponded with volcanism of this area might be regarded as subduction related.

6. Conclusions

The Popa area lies in the Kyaukpadaung Township, Myingyan District in Mandalay Region. Mt. Popa is a stratovolcano in central Myanmar. Mt. Popa could have had an eruption in 442 BCE.

Microscopically, the main common textures of the studied samples are porphyritic, glomerophyritic, intergranular, ophitic to sub-ophitic, radiate and seriate textures. Based on the modal composition of minerals, andesites of the study area can be divided into augite-hornblende phyric andesite, olivine-augite phyric andesite, hypersthene-hornblende- augite phyric andesite, and augite phyric andesite.

Under the microscope, the plagioclase crystals are the predominant minerals and occur both in phenocrysts and microcrystalline groundmass. The zonal arrangement of minute melt inclusions in plagioclase suggests that the several stages in the growth of plagioclase crystals. Rarely, orthoclase occurs as phenocrysts in some samples with plagioclase and hornblende. Hornblende occurs as major amphibole mineral in andesites of the study area. Hornblende has euhedral to subhedral long prismatic form. Augite occurs mostly as megacryst or phenocryst, microphenocryst as well as in groundmass. It is eight-sided euhedral to subhedral, up to 1.5mm in diameter and fresh prismatic crystal. Olivine occurs as minor amount in the andesites of the study area. Petrographically, most of the olivine gives six-sided euhedral to subhedral phenocrysts, colorless, high relief and parallel extinction. Hypersthene occurs as phenocrysts in some samples. Under microscope, magnetite is found as black opaque, anhedral grain as microphenocryst and groundmass. Iddingsite, clay minerals and chlorite are found as secondary minerals in andesites of the study area.

Plagioclase microcrystalline laths exhibit pilotassitic texture, the sub-parallel arrangement amongst them giving trachytic texture and becomes a reference in telling the existence of lava flow processes when rock formation. Zoning in plagioclase is formed due to pressure and temperature change during magma raising and volatile release during magmatic eruption which causes plagioclase compositional differentiation Ophitic and sub-ophitic texture of augite-hornblende phyric andesite indicates the coprecipitation of plagioclase with pyroxene. Flow texture in andesite of the study area reflects that the magma was moving at the time of solidification. The black iron-oxides often seen around the edge of Oxo-hornblendes result from resorption effects.

The analytical results of the studied samples are plotted in Total Alkali-Silica (TAS) diagram which indicate that the most of samples fall in the andesite and basaltic andesite fields. The total alkali vs. silica diagram show that the andesite samples dominantly plot within subalkaline field. Data plotted on the AFM diagram clearly indicate that almost all of the andesites fall in the field of calc-alkaline series. Al-Mg-Fe^T+Ti ternary diagram, most of the studied samples plotted within the andesite field of calc-alkaline series.

Based on K_2O, TiO_2, and P_2O_5, origin of andesites related to continental crust. According to diagram of TiO_2, 10xMnO, and 10xP_2O_5, all analyzed andesite samples related to Island Arc-Calc Alkaline Series. The studied andesites have been erupted in volcanic arc setting indicated by tectonic discrimination diagram including Zr versus Ti (Pearce,1982). According to the above mention geochemical facts and discriminant diagrams point out that all the studied samples fall within the field of volcanic arc. These characters are corresponded with volcanism of this area might be regarded as subduction related.

7. Acknowledgements

I would like to express my sincere gratitude to Magway University, especially my supervisors and professors, for their guidance and support during my MSc program where this research was originally conducted. I am deeply grateful to the Managing Director and officials of Myanma Gems Enterprise for granting me permission to participate and present this paper. Furthermore, I wish to extend my heartfelt thanks to the Forest Department for organizing this paper reading session and providing me with the opportunity to share my research findings. Finally, I thank everyone who contributed to the successful completion and presentation of this study.

8. References

Aung Moe, 1980. Petrology and Structures of the rocks of mount Popa Area, Kyaukpadaung Township. *Unpublished M.Sc Thesis, Yangon University.*

Barker, A.J., 2014. *A key to identification of rock-forming minerals in thin-section*, CRC Pres, Taylor & Francis gp, London, Uk, pp.182.

Belousov A., M. Belousova, Khin Zaw, M.J. Streck, I. Bindeman, S. Meffre, P. Vasconcelos, 2018. Holocene eruptions of Mt. Popa, Myanmar: Volcanological evidence of the ongoing subduction of Indian Plate along Arakan Trench. *Journal of Volcanology and Geothermal Research 360. 126–138.*

Chhibber, H.L., 1934. *Geology of Burma*. McMillan, London (538 pp)

Cox K.G., & Bell J.D., & Pankhurst, R.G., 1979. *The interpretation of igneous rocks*. George, Allen and Unwin, (Publisher), Ltd. P450.

Deer, W.A., R.A. Howie, J. Zusman, 2013. *Rock forming minerals*, 3rd ed., Licensing Angency Ltd.

Hla Min, 2020. Petrochemical Study on the Volcanic Rocks from the Different Lava Flows of the Popa Area, Kyaukpadaung Township, Mandalay Region. *Meiktila University Research Journal, 2020, Vol. XI, No.1.*

Irvine, T. N. & Baragar, W. R. A., 1971. A guide to the chemical classificstion of the common volcanic rock, Canadian journal of Earth Sciences, 8 (5): 523-548.

Jensen L.S.,1976. A new cation plot for classifying subalkalic volcanic rocks. Min Nat Resources Ontario Division of Mines Misc paper 66: 20.

Jerram D A, Dobson K J, Morgan D J, Pankhurst M J. 2018 The petrogenesis of magmatic systems: using igneous textures to understand magmatic process *Volcanic and Igneous Plumbing Systems* Steffi Burchardt (Amsterdam: Elsevier) chapter 8 pp 191-229

Johannsen, A., 1939. A descriptive petrography of the igneous rocks, *University of Chicago*.
Keer, P.F., 1977. *Optical Mineralogy,* 4th ed., McGraw-Hill Book Company, pp.285-383

Khin Maung Hla and Htin Lynn Aung, 2018. Geomorphology of Mount Popa and its Environs, Kyaukpadaung Township, Mandalay Region, *Bago University Research Journal, 2018, Vol. 8, No. 1*.

Lee, H.Y., Chung, S.L., Yang, H.M., 2016. Late Cenozoic volcanismin central Myanmar: geochemical characteristics and geodynamic significance. *Lithos 245*, 174–190.

Mackenzie, W.S, and C. Gulford, 1980. *Atlas of rock forming minerals in thin section*, Taylor & Francis Gp.

Mar Mar Khaing and Maw Maw Myint, 2020. Rock Sequences and Petrography of the Popa – Kyauktaga Area, Kyaukpadaung Township, Mandalay Region. *Meiktila University Research Journal, 2020, Vol.XI, No.1*.

Marin, J., Muhammad, Y.M. and Winarno, T., 2022. Characteristics of volcanic rocks and associated intrusions based on petrography analysis in Jari-Krondonan Area, Bojonegoro Regency, East Java. *IOP Conference Series: Earth and Environmental Science.1047 012034*.

Maung Thein, 2000. Summary of the geological history of Myanmar. *Unpub*.

Maury, R.C., Pubellier, M., Rangin, C., Wulput, L., Cotten, J., Socquet, A., Belon, H., Juillaud, J.-P., Htun, H.M., 2004. Quaternary calc-alkaline and alkaline volcanism in an hyperoblique convergence setting, central Myanmar and western Yunnan. *Bull. Soc. Geol.* Fr. 175 (5), 461–472.

Maw Maw Myint, 2009. Natural Pozzolan in Mount Popa Area. *Meiktila University Research Journal, Vol. II, No.1*.

Mitchell, A.H.G., Chung, S.L., Oo, Thura, Lin, T.H., Hung, C.H., 2012. Zircon U–Pb ages in Myanmar: magmatic–metamorphic events and the closure of a neo-Tethys ocean? *J. Asian Earth Sci*. 56, 1–23.

Mullen, E.D. (1983) MnO/TiO2/P2O5: A Minor Element Discriminant for Basaltic Rocks of Oceanic Environments and Its Implications for Petrogenesis. Earth and Planetary Science Letters, 62, 53-62. https://doi.org/10.1016/0012-821X(83)90070-5

Muller, D., & Groves D.l. 1997: Potassic igneous rock and associated gold-copper mineralization. *Lecture Notes in Earth Sciences*. No.56.

Muller, D. and Groves, D.I., 2016. Poatssic igneous rocks and associated gold -copper mineralization; *springer Berlin, Germany*, p. 238.

Myanmar Geosciences Society (MGS), 2014, Geological Map of Myanmar: scale 1:2250000, 1sheet.

Nelson S T, Montana A .1992 Sieve-textured plagioclase in volcanic rocks produced by rapid decompression *American Mineralogist* **77** 1242-49

Newhall, C.G., Self, S., 1982. The volcanic explosivity index (VEI) an estimate of explosive magnitude for historical volcanism. *J. Geophys. Res. Oceans Atmos*. 87 (C2), 1231–1238.

Ni.,J.F., Guzman- Speziale, M., tlolt, M.E, Wallace, T.C., & Seager, W.R., 1989. Accretionary tectonics of Burma and the three dimensional geometry of the Burma Subduction Zone Geology, *vol.17, pp 68- 71.*

Pearce, J.A., & Cann, J. R., 1973, Tectonic setting of basic volcanic rocks determined using trace element analyses. *journal of Earth and Planetary Science Letters*, 19, 290-300.

Pearce, T.H., Gorman, B.E. and Birkett, T.C, 1977. The relationship between major element geochemistry and tectonic environment of basic and intermediate volcanic rocks, Earth and Planetary Science Letters 36, 121-132.

Pivnik, D.A., Nahm, J., Tucker, R.S., Smith, G.O., Nyein, Kyaw, Nyunt, Maung, Maung, Hla, 1998. Polyphase deformation in a fore-arc/back-arc basin, Salin subbasin, Myanmar (Burma). *AAPG Bull.* 82 (10), 1837–1856.

Rollinson, H.R., 1995. *Using geochemical data: evaluation, presentation, interpretation*. Wiley, New York, 325p.

Seaman S J. 2000 Crystal clusters, feldspar a glomerocrysts, and magma envelopes in the Atascosa Lookout Lava Flow Southern Arizona, USA: recorders of magmatic events *Journal of Petrology* 41 issue 5 693-716

Sen G. 2014 *Petrology: Principles and Practice* (Berlin: Springer) p 359

Shervais, J.W. (1982) Ti-V Plots and the Petrogenesis of Modern and Ophiolitic Lavas. *Earth and Planetary Science Letters*, 59, 101-118.https://doi.org/10.1016/0012-821X(82)90120-0

Si Thu Aung, 2009. Petrology of the Mt. Popa, Kyaukpadaung Township. *Unpublished M.Sc Thesis, Magway University*.

Stephenson, D. & T.R. Marshall,1984. The Petrology and mineralogy of Mt. Popa Volcano and the nature of the Late-Cenozoic Burma volcanic-Arc, *Geol. Soc. London, Vol. 141*.

Suhada, R.A. and Dyah Hastuti, E.W, 2019. Petrogenesis study of quaternary volcanic rocks based on petrography analysis in Lubuk NipisVillage, Muara Enim District, South Sumatra. *IOP conference series: material science and Engineering*.

Yogodzinski, G.M., Lees, J.M., Churikova, T.G., Dorendorf, F., Woerner, G. and Volynets, O.N. (2001) Geochemical Evidence for the Melting of Subducting Oceanic Lithosphere at Plate Edges. *Nature, 409*, 500-504. https://doi.org/10.1038/35054039